Journal of Solid Mechanics Vol. 14, No. 3 (2022) pp. 332-344
DOI: 10.22034/jsm.2021.1921808.1675

Research Paper

Static Analysis and Fatigue of DHS Implants to Treatment Femoral and Intertrochanteric Neck Fractures Using Ti6Al4V and SS316 Alloys, A Finite Element Analysis

A. Shokrgozar Navi [1], S. Etemadi Haghighi [1,*], M. Haghpanahi [2], A. Momeni [3]

[1] *Department of Mechanical Engineering, Science and Research Branch, Islamic Azad University, Tehran, Iran*
[2] *Department of Mechanical Engineering, Iran University of Science and Technology, Tehran, Iran*
[3] *Materials Science and Engineering Department, Hamedan University of Technology, Hamedan, Iran*

Received 26 May 2022; accepted 1 July 2022

ABSTRACT

The neck fractures and the femurs intertrochanteric are common complications that are recovered by a multicomponent implant called dynamic hip screw (DHS). In the present study, a standard four-hole DHS with Ti6Al4V (Ti6) and SS316l (SS) alloys for static mode (slow walking) and fatigue mode like normal walking (NW), descending stairs (DS), and falling (FA) by finite elements analysis (FEA) have been evaluated (ANSYS software). The results have been confirmed by similar studies in static mode and maximum Von Mises stress and strain are obtained for Ti6 about 145 *MPa* and 0.191%, and SS about 196 *MPa* and 0.121%. Most critical stress points occur in cortical screws, plate holes, compression screws, and lag screws, respectively. DHS components with Ti6 alloy have infinite life in NW and DS, also in FA, they have a finite life (10^7-10^8 cycle) with alternating Von Mises stress ($\sigma_{a\max}$) ~ 425 *MPa*, while for SS they have finite life in all activities, which NW ~10^7 cycle, DS~10^6 cycle, and even in FA cortical screw life of failure reaches to 98 cycles and $\sigma_{a\max} = 486 Mpa$. The critical regions are the same as the failure regions common in biomechanical and clinical studies. These regions are mainly concentration stress points that lead to DHS failure as the crack grows.

Keywords : DHS; Intertrochanteric; Fatigue; Femur; Finite elements.

1 INTRODUCTION

TODEY, femoral fractures have increased dramatically due to the increasing number of elderly people in various communities and accidents. Dynamic hip screw (DHS) is used to repair minor fractures and cracks in

*Corresponding author. Tel.: +98 21 44865202.
E-mail address: setemadi@srbiau.ac.ir (S. Etemadi Haghighi)

the femoral neck, intertrochanteric and subtrochanteric regions, where the fracture line passes through both the large and small the femur trochanters. The extension of DHS from near the femur head to the middle parts of the femur causes the distribution of stress to be transmitted to more parts, thus preparing the fractured area by fixing the lag screw for the repair and ossification. Failure to repair the fracture or improper welding of the injured area causes necrosis and bedsores and causes severe injuries to the patient. The main reason of failure implants is the fatigue materials due to their location in places that are constantly under the influence of force [1]. According to research and human physics, the femur is a point that is most susceptible to various complications. Today, titanium alloys (Ti6Al4V) and stainless steel alloys (SS316l) are used to make DHS implants. The mechanical properties of alloys have a great impact on their service life. Ti6Al4V with high strength and good fatigue and corrosion resistance has found many applications in medicine [2-5]. SS316l, which is widely used in bone implants, also it has good fatigue and strength properties in medical applications [6-9]. However, few studies have been done on DHS in terms of fatigue, which have also been laboratory [10-13]. Exposure to frequent and varied forces (fatigue) in dental implants is one of the main causes of failure [14, 15]. The geometric shape and the number of holes in the plate are the factors that can change the amount of stress in DHS [16]. The examination of fatigue in different parts of DHS such as lock compression plate [10], lock plate [11, 12], and sliding plate [17, 18] shows that failure in DHS can be due to weakness in geometry, surgery, and alloy. Also, optimization with a fatigue approach for holding plates [19, 20] can help to remove some problems in DHS design. Applied forces to DHS depend on the physique and the type of ossification of each person like weight, skeleton, muscles, and the type of activity of the target organ. The amount of force and torque applied to the femur is examined by Bergmann [21, 22] for movements such as standing, walking, running, going up and downstairs, and other activities. The same research has been developed by Farhoudi et al [23] and also the place of the effect of weight and muscle forces that are very effective in the amount of stress on the femur has been studied in research [21-27] in the laboratory and software. Also for activities such as falling [28], values are included as the amount of force on the femur. Bone is essentially an anisotropic material [29-31] but, in a lot of studies [10-12, 27, 32-36], it is thought isotropic material due to its similar behavior in the macroscopic state. A lot of finite element analysis (FEA) has been performed on DHS in static mode to investigate failure points. Examining the biomechanical behavior of the femur to understand better is a difficult task because the femur varies in shape, material properties, geometry, porosity, density, and the femur is a living part that is always changing. FEA can cover the effects of linear and nonlinear analysis together and consider the effects of geometry, time, and different states.

In this study, because DHS (Fig. 1(a)) is subjected to frequent and heavy loads to eliminate the effects of the femoral neck and intertrochanteric fractures (Fig. 1(b)), the average of acting forces on the femur (according to previous research) in various activities is considered. Then by designing the femur and DHS (four holes standard) in Solid Works software and assembling in Commercial finite element analysis software for two alloys SS316 (SS) and Ti6Al4V (Ti6), of finite element analysis (FEA) in static mode (very slow walking) and fatigue analysis such as normal walking (NW), downstairs (DS) and falling (FA) have been performed. The critical points, alternating stress and life (cycle) of the components have been calculated and compared with similar research in static, and fatigue (laboratory) modes.

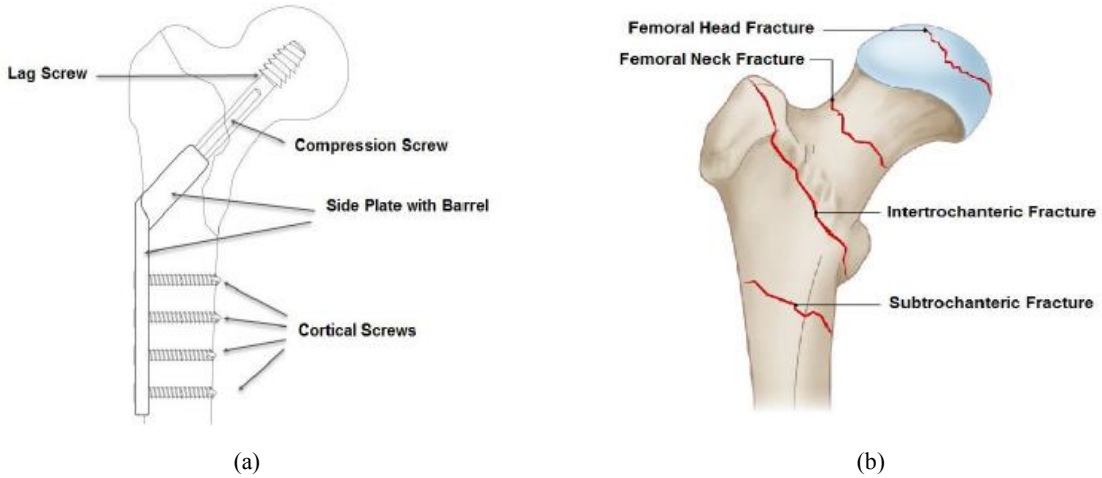

(a) (b)

Fig.1
The ideograph of the (a) dynamic hip screw and (b) fractures of the femur.

2 MATERIALS AND METHODS

2.1 Application materials

In the present study, the femur is assumed to be an inhomogeneous and anisotropic material (orthotropic) with the properties of Table 1, whose bone properties differ in different directions [31]. Its mechanical properties are the function of the location and the direction in which the force is applied. The stiffness in the axial direction is about twice bigger than in the radial direction and the axial limit deformation of the bone is twice higher than the radial one. In the trabecular (middle) part of the bone, where the bone tissue is softer, the value of Young's modulus is low, and in the cortical part, its mechanical properties are at a higher level.

Table 1
Mechanical properties of femur and DHS [31].

Part&Materials	$E(GPa)$ trabecular	$E(GPa)$ cortical			$\sigma_y\ \sigma_{uts}$ (MPa)	ϑ trabecular	ϑ cortical		
		E_1	E_2	E_3			ϑ_1	ϑ_2	ϑ_3
Femoral head	0.9	12	13.4	20	80,100	0.29	0.376	0.222	0.234
In-trochanteric	0.26	12	13.4	20	80,100	0.29	0.376	0.222	0.234
Femoral shaft	-	12	13.4	20	100,120	-	0.376	0.222	0.234
Femoral Neck	0.62	12	13.4	20	75,95	0.29	0.376	0.222	0.234

Also, the specifications of SS and Ti6 alloys, which are common in the manufacture of medical implants, are shown in Table 2 [2-9]. Alpha/beta ($\alpha+\beta$) Ti–6Al–4V (Ti6) alloy has been widely used in the medical industry, because of its high specific strength, good balance of strength, ductility, weld ability, and corrosion resistance. The Young's modulus range is about (110-125 *GPa*) and fully reversed axial fatigue tests performed at ambient temperature shows that alternating stresses (σ_a) from 850 *MPa* at low cycles (less than 10^3) to 420 *MPa* at high cycles (10^9) are shown in Table 2 [2-5]. Type 316L stainless steel is one of the important medical structural materials that is made primarily of iron and carbon in a two-step process. Although the mechanical and biological properties of this alloy are less than Ti6, economic conditions and having minimal properties have made it one of the most widely used medical alloys. The Young's modulus is in between 185 to 210 *GPa* and the yield strength (σ_y) is 380-700 *MPa* in its various grades. The fatigue properties of SS for σ_a from 494 *MPa* at low cycles (10^3) to 220 *MPa* at high cycles (10^9) are shown in Table 2 [6-9]. The S-N curve (Fig. 2) shows the rate of material resistance (alternating stress) to a life of failure (cycles) where the alternating stress (σ_a) of Ti6 alloy is higher than SS.

Table 2
Mechanical properties of DHS [2-9].

Materials	E (GPa)	σ_y (MPa)	σ_{uts} (MPa)	ϑ	$\sigma_f\ in 10^1$ (MPa)	$\sigma_f\ in 10^2$ (MPa)	$\sigma_f\ in 10^3$ (MPa)	$\sigma_f\ in 10^4$ (MPa)	$\sigma_f\ in 10^5$ (MPa)	$\sigma_f\ in 10^6$ (MPa)	$\sigma_f\ in 10^7$ (MPa)
Ti6Al4V(Ti6)	110	850	880	0.34	830	815	790	695	580	520	393
SS316(SS)	193	494	661	0.31	490	460	435	415	390	360	220

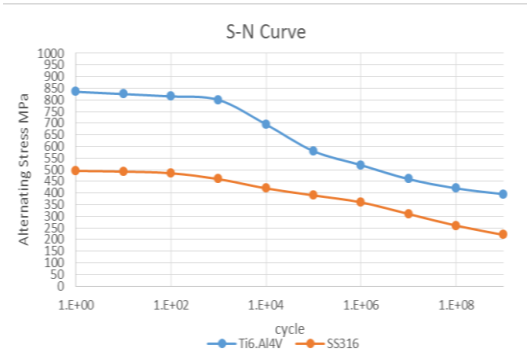

Fig.2
S-N curve of Ti6, SS [2-9].

2.2 Modeling in finite element software

A standard right leg femur [28] for a person weighing 750 *N*, along with a standard four-hole DHS [28, 37], is designed for implantation in the neck and intertrochanteric femur in 3D modeling software. The four-hole DHS implant has four main parts including lag screw, plate, compression screw, and cortical screws, which are shown in Fig. 3(a). The lag screw part transfers the load applied to the femoral head to the plate and the middle part of the femur. The compression screw makes the dynamic mode possible, and these two parts are usually called the main screw. Also, the plates are classified according to the number of their holes, which play a significant role in obtaining the critical point [19]. Cortical screws are also responsible for fixing the entire DHS in the femur. Designs for assembly, loading, and creating border conditions have been included in the software. The DHS implant is placed inside the femur at an angle of 135 degrees parallel to the bone (Fig.3), so the lag screw with a compression screw at the same angle is placed parallel to the femoral neck in the middle cortex of the femoral head. This analysis was performed with 1173255 nodes and 802331 elements and 2 *mm* mesh for bone and 1.5 *mm* for DHS of 8-node element type.

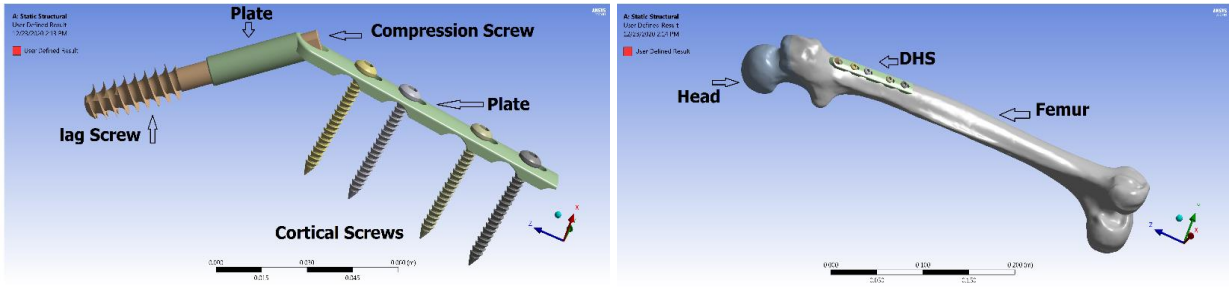

(a) (b)

Fig.3
Assembly in software (a) DHS implant (b) DHS assembly in the femur.

2.3 Applying force and boundary conditions for static mode

Four forces are applied to the femur bone [16,17,21-30], which include Joint reaction (JR), Abductors (AB), Vastus lateralis (VL), and Iliopsoas (IL), and the amount of forces in the different movements was based on the weight of people. In the present study, the modes of slow walking (SW), normal walking (NW), descending stairs (DS), and falling (FA), according to the conditions of Table 3, are considered based on the comprehensive research of Bergmann [21, 22] and [23-27]. Table 3 shows the amount, location, and angle of incoming forces in different modes. Since SW is like standing on one leg (static position), an average value (SW) is considered for it, which is the result of mining from research mentioned forces (PS), Bergmann research (BG) for slow walking, and 2D analysis [27] performed in this study.

Table 3
Distribution of the four forces entering the femur**.**

Load case	Force	*x* (*mm*)	*y* (*mm*)	*z* (*mm*)	φ	γ	*F* (BG) (W %)	*F* (2D) (W %)	*F* (PS) (W %)	*F*(SW) (W %)	*F*(NW) (W %)	*F*(DS) (W %)	*F*(FA) (W %)
Joint reaction (JR)	P_1	-44	408	32	159	7	252	264	265	257	288	316	495
Abductors(AB)	P_2	8	360	31	20	180	101	121	82	110	102	124	162
Vastus lateralis(VL)	P_3	-8	316	29	47	262	40	-	25	33	40	45	48
Iliopsoas(IL)	P_4	-29	316	36	180	-	43	-	29	36	46	49	52

According to Table 2 and Fig. 4, among the four forces acting on the femur, the JR has the highest value and with a range between 2.58 to 4.95 weights (W %) per person, on the femur in the position of SW, NW, DS, and FA enter. In addition, the JR force is affected by various parameters such as the type of ossification and upper torso of persons which can have a longer torque arm by angling the femur to the body, and other forces are also affected; the same is true for the abductor force. The AB force is formed according to the JR, which is about 30 to 45% of the JR force and its amount varies between 1 to 1.6 weights of each person. The muscular forces of the femoral part of the VL and IL, the values of which have been calculated in research [21-26], for different activities, are in the maximum

state between 0.25 and 0.52 by weight. Obviously, the amount of muscle force is not always within this range and decreases with the type of activity. Falling activity (FA) puts about 4.6 to 5.2 times the weight of each person on the femur, which is the most force among the activities [28]. The effect of torque on the femur has also been neglected in this study. This design is based on the stress life criterion, and the amount of static stress is calculated based on the Von Mises criterion. The femur is assumed to be fixed according to Fig. 4a of the condylar part under boundary conditions.

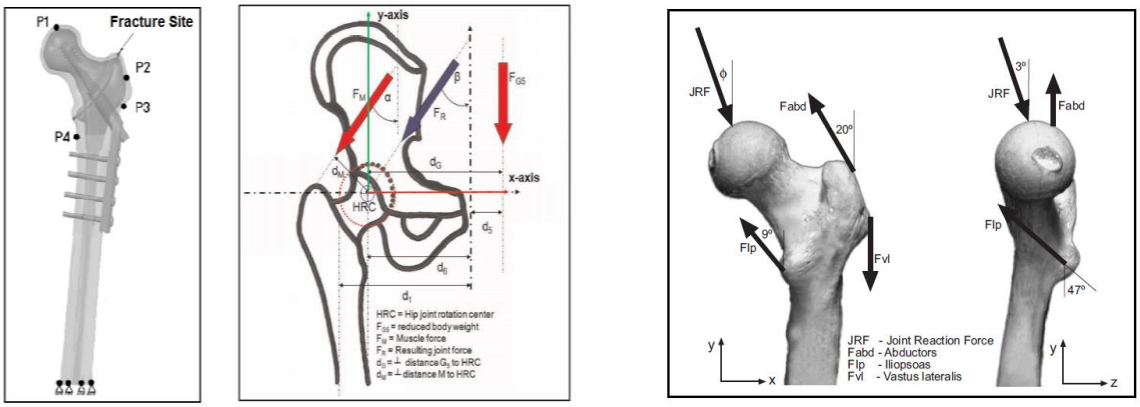

(a) (b) (c)

Fig.4
Type of forces on the femur with DHS (a) Schematic of forces and support [16], (b) Schematic in two-dimensional mode [27] ,(c) Location and angle of application of forces [24].

2.4 Fatigue analysis

Fatigue analysis is a post-static analysis and is performed by assuming the static mode conditions, different movement conditions, the frequency of movement, and the amount of force applied. The criterion to evaluate the stress behavior is stress life, and the modified Goodman criterion is used to estimate the life of DHS components. Because bone is a living element and changes with nutrition and over time; in the present study, femur bone has not been examined for fatigue and the fatigue properties only include DHS implants. The Cycle time (interval) for SW is 1.25 seconds, for NW is 1.11 seconds, and for DS is 1.46 seconds [21], and for FA is 0.96 seconds.

3 RESULTS

3.1 Static analysis results

Table 4 shows the results of the static analysis to stand (like SW activity) in both alloys. These results are obtained from 5 time runs in software and the cortical screws (especially zone 5) show the most critical points. Also, the compression and lag screw have the least amount of stress on the DHS. The femur has the least amount of stress in the head, but in some places, such as intertrochanteric appendages, the concentration points have high stresses. In addition to presenting the maximum amount of stress in specific parts of the implants, which is shown with numbers 1 to 6 in Fig. 5 and 6, the average amount of stress on each part is also shown in Table 4. Fig. 5 shows the stress distribution contours for Ti6 and Fig. 6 represent the strain distribution in this alloy. The maximum stress and strain trends for both alloys in Table 4 indicate that the SS alloy has a lower strain than the Ti6 alloy. Also, Fig. 7 shows the distribution of strain in different parts of the bone and the DHS with Ti6, which is the highest strain in the bone in the trochanteric region and then in the cortical screws. In some articles (like [35]), screws are assumed to be threadless (in practice, this never happens), which causes these members to become out of critical condition.

Table 4
Distribution of stress and strain in the DHS and bone for SW activity.

Part	Avg Stress V-M(*MPa*) Ti6	Max Stress V-M(*MPa*) Ti6			Max Stress V-M(*MPa*) SS			Max Strain (%) Ti6			Max Strain (%) SS		
	present	present	[28]	[35]	present	[16]	[28]	present	[28]	[35]	present	[16]	[28]
Bone head	3	32	33	-	32	-	33	0.255	0.195	-	0.265	-	0.195
Bone body	9	38	33	-	38	-	33	0.271	0.195	-	0.277	-	0.195
Lag screw	28	121	17	250	150	159	23	0.148	0.020	0.227	0.103	0.106	0.073
Cortical	51	134	19	-	167	-	16	0.169	0.021	-	0.107	-	0.075
Cortical	58	137	25	-	172	-	27	0.178	0.022	-	0.109	-	0.079
Cortical	68	145	65	-	196	-	87	0.191	0.054	-	0.121	0.124	0.088
Cortical	54	143	24	-	191	321	17	0.183	0.022	-	0.118	0.165	0.084
Plate	62	138	54	280	175	91.5	68	0.179	0.048	0.254	0.111	0.085	0.081
Compressio	41	124	47	-	155	-	47	0.153	0.043	-	0.105	-	0.071

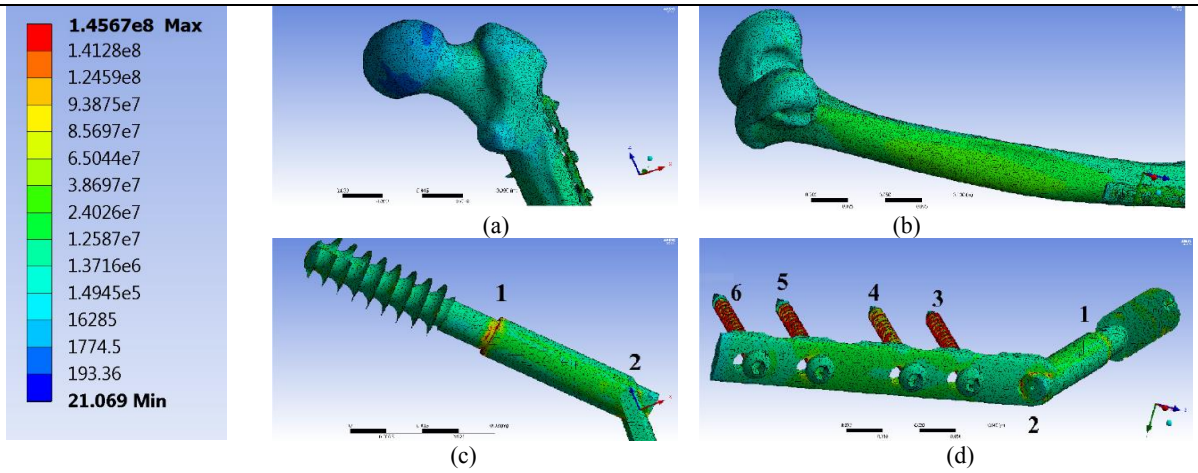

Fig.5
Von Mises Stress distribution in DHS (Pa) for Ti6 (a) femur Head (b) femur and lower condyle (c) lag screw (d) plate and cortical screws.

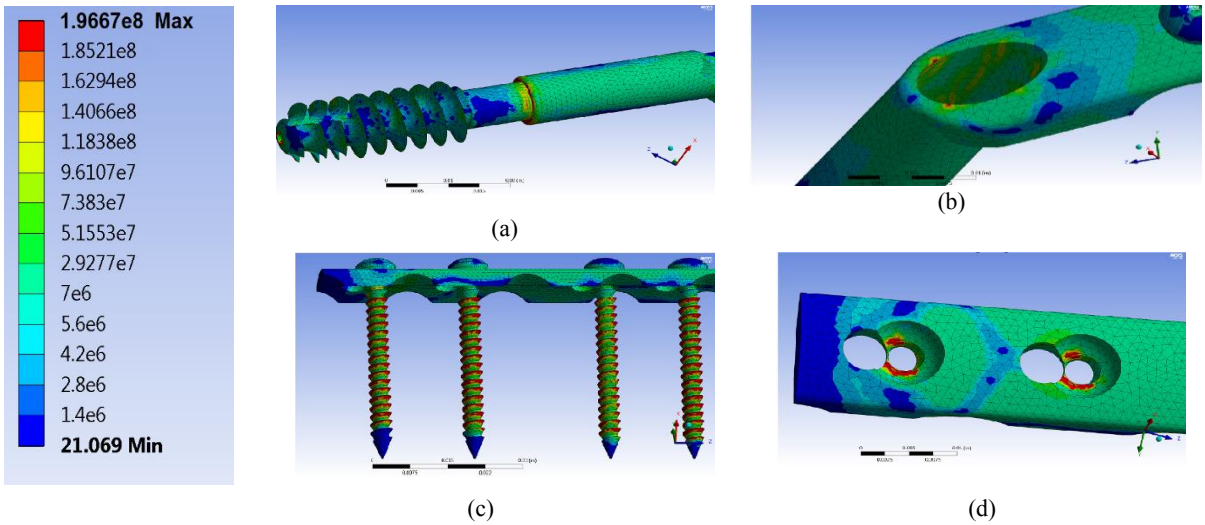

Fig.6
Von Mises Stress distribution in DHS (Pa) for SS (a) lag screw (b) plate in compression screw region (c) plate and cortical screws (d) plate in holes region.

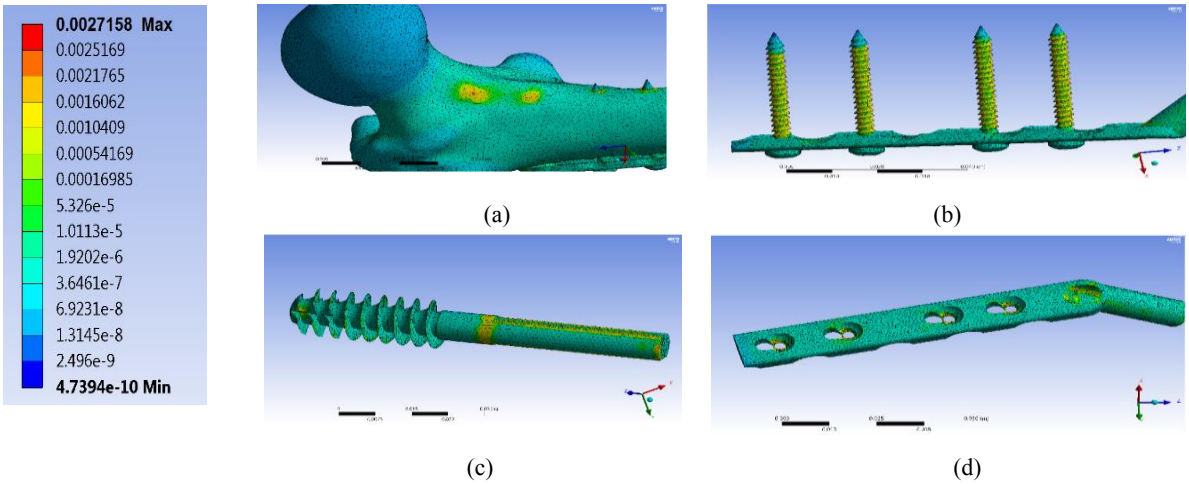

Fig.7
Strain distribution (*m/m*) for Ti6 in critical points on (a) on femur (b) cortical screws (c) lag screw (d) plate.

3.2 Fatigue analysis results

The results obtained from the fatigue analysis by FEA indicate the repetition of critical points such as the static part (Table 5). However, the type of loading on the life of the components is very influential. In the present study, Fatigue analysis was performed for three motion models (NW, DS, FA), while it was predictable that by increasing and changing the type of load, the life of components will be reduced from indefinite (∞) to finite life (less than 10^9cycles). Table 5 shows that alloys can reduce or increase the life of the components, which is obvious. Lag screw as the main part that is responsible for maintaining the damaged part and according to Table 5 in triple activity has the longest life. This part by changing the type of activity withstands maximum alternating stress ($\sigma_{a\max}$) of about 135 to 328 *MPa* in Ti6 and 189 to 328 in SS, which has an infinite life in Ti6 (all activity) but for SS it has a finite life (less than 10^9cycles) in DS and FA modes.

The plate is the main DHS holder, which relatively long organ located both inside and outside the bone, with $\sigma_{a\max}$ 210 to 418 *MPa* for Ti6 and 272 to 483 *MPa* in SS Alloy. This part in NW with Ti6 has infinite life, but, in other activities for both alloys, it has a finite life. However, the life ratio in the Ti6 is better than the SS and, in some places, the life of components reaches about 109 cycles which cortical screws and holes are critical points with a short life (Fig. 8, 9). Cortical screws are highly exposed to cyclic stresses and their lifespan has been observed in the low range, which has been well demonstrated in [12], and zone 5 (Fig.5(d)) is the most critical point (98 cycles). This screw has infinite life in NW for Ti6, but other activities in both alloys have a finite life; also other cortical screws have similar conditions. For all cortical screws, $\sigma_{a\max}$ is from 178 to 425 *MPa* for Ti6 and 241 to 486 *MPa* for SS. The threaded edges of the cortical screws, which are the concentration stress points, and the tips of the cortical screws have the least stress because they remain in the muscle space. The compression screw belongs to the lag screw that creates dynamic action and transfers contact force to the plate and the body of the femur. Also $\sigma_{a\max}$ from 161 to 348 *MPa* for Ti6 and 215 to 415 *MPa* for SS indicated that this part is one of the safety components in DHS. This part is only in the case of DS and FA with SS alloy in the finite life range.

Table 5
Results of DHS implant fatigue analysis (average lifespan for 5 times analysis).

Part/action	Normal Walking(NW)				Down Stair(DS)				Falling(FA)			
	$\sigma_{a\max}$ (*MPa*)		Life(cycle)		$\sigma_{a\max}$ (*MPa*)		Life(cycle)		$\sigma_{a\max}$ (*MPa*)		Life(cycle)	
Alloy	Ti6	SS	Ti6	SS	Ti6	SS	Ti6	SS	Ti6	SS	Ti6	SS
Lag screw	135	189	∞	∞	168	228	∞	8.1×10^2	328	388	∞	4.1×10^2
Cortical screw1	185	249	∞	3.3×10^2	223	291	∞	4.5×10^7	397	452	9.7×10^2	3.31×10^2
Cortical screw2	198	267	∞	8.2×10^7	235	319	∞	8.4×10^6	411	472	5.2×10^2	2.95×10^2
Cortical screw3	232	292	∞	4.6×10^7	285	338	∞	5.1×10^6	425	486	9.1×10^7	9.8×10^2
Cortical screw4	178	241	∞	5.1×10^2	215	301	∞	3.9×10^7	405	468	7.5×10^2	3.25×10^2

Plate	210	272	∞	6.3×10^{7}	275	320	∞	8.3×10^{6}	418	483	1.6×10^{2}	1.09×10^{2}
Compression screw	161	215	∞	∞	192	258	∞	1.1×10^{2}	348	415	∞	2.1×10^{4}

For Ti6 alloy the contours of the fatigue life distribution (Fig. 8) and alternating stress distribution (Fig. 9) indicated that life is in the infinite range in a lot of places of DHS but some points like concentration stress points are under shorter life and higher stress.

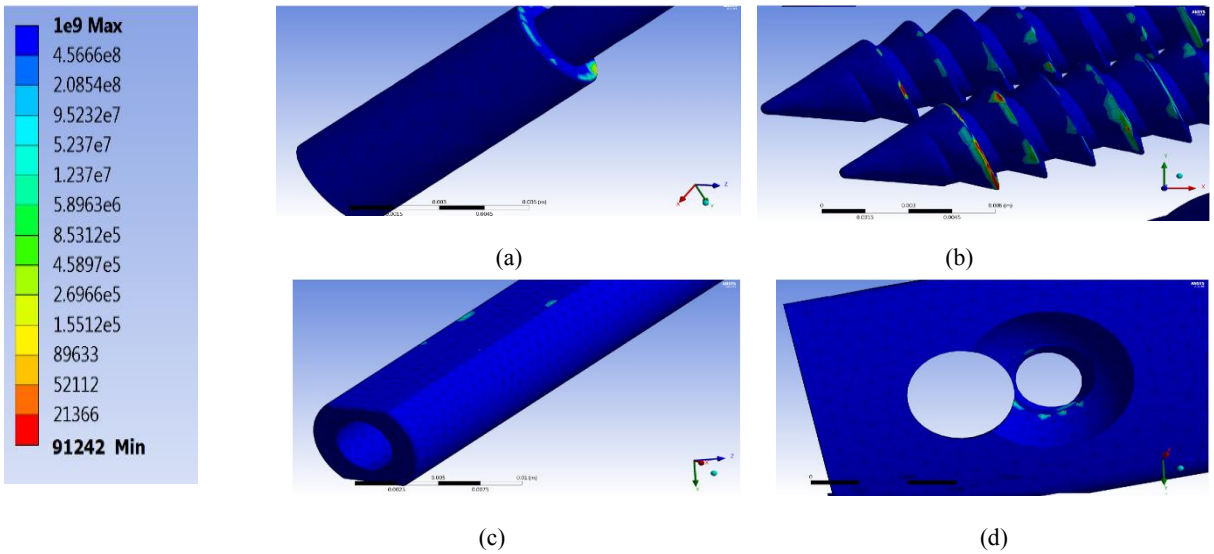

Fig.8
Distribution of Fatigue life in Ti6 alloy (cycle), (a) compression screw (b) cortical screw in thread regions (c) lag screw (d) plate in hole regions.

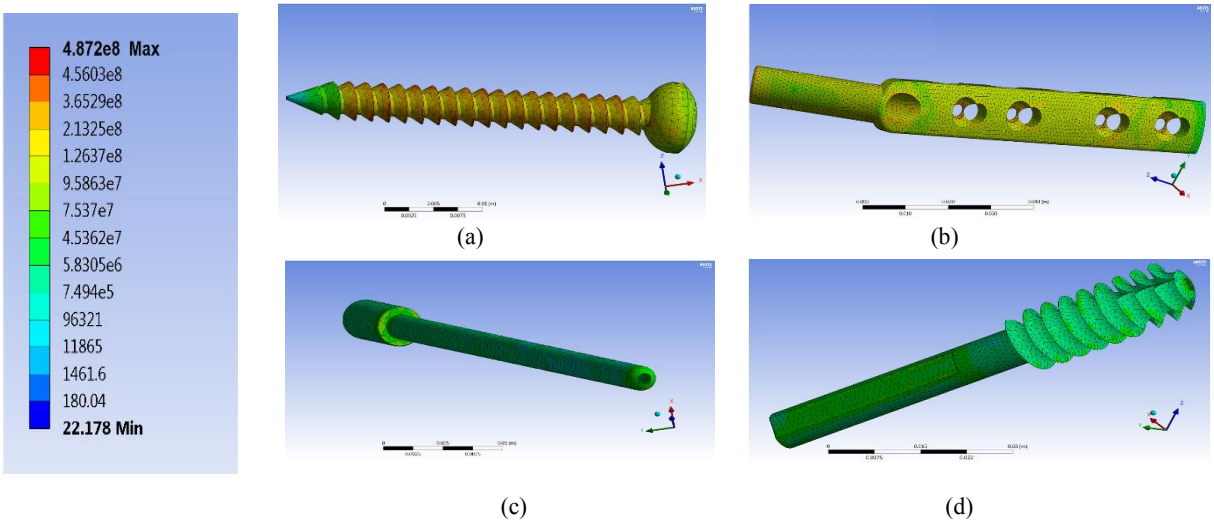

Fig.9
Distribution of alternating stress in DHS implants (*MPa*) (a) cortical screw (b) plate (c) compression screw (d) lag screw.

4 ANALYSIS OF RESULTS

4.1 Static analysis

Much research has been done on DHS by FEM, but they all differ in some subjects as the type and amount of force applied to the femur, the geometry of the DHS and bone, the model of the DHS and bone, the boundary conditions,

alloys, isotropy or anisotropy of bone and the age of patients make it almost impossible to examine the two studies together in terms of stress and strain, so more research is in case reports and differences in results are inevitable. However, in other cases, the trend of changes in different phenomena can be evaluated and compared. The stress concentration caused by the screw layout of the implanted plate is one of the main reasons for the fracture or failure in DHS [19]. Fig. 10 shows the different models of DHS failures in different conditions. They most often occur at concentration stress points such as screw threads (3-6 zone in Fig. 5(a)), lag screw edges (zone 1 in Fig. 5(c)), and plate holes (zone 2 in Fig 5(c) and Fig. 6(d)). These problems can be solved by repairing them during implant manufacturing or coexisting with the bone. As shown in Fig. 7, 8 most points of the DHS have a very low average σ_a (Table 5). The amount of strain on the components depends on the E of the alloy and applied stress, so the amount of strain in the Ti6 is slightly higher than SS. On the other hand, the amount of strain in the bone (due to the low yang modulus) is 0.27% that is higher than the implant components. The most strain occurs in the neck, which is shown as a concentration stress point (Fig. 7(a)). Several regions of bone have been observed, like condyle and femoral shaft with a strain between 0.1 to 0.23 %. According to Figs. 7 and the results of Table 4 in both alloys, the maximum Von Mises strain (ε_{V-Max}) for cortical screws are between 0.107-0.191%, in plate 0.111-0.179%, in lag screw 0.105-0.153% and in compression screw 0.103-0.148%, while the amount of ε_{V-Max} in the SS is between 35 to 52% lower than Ti6.

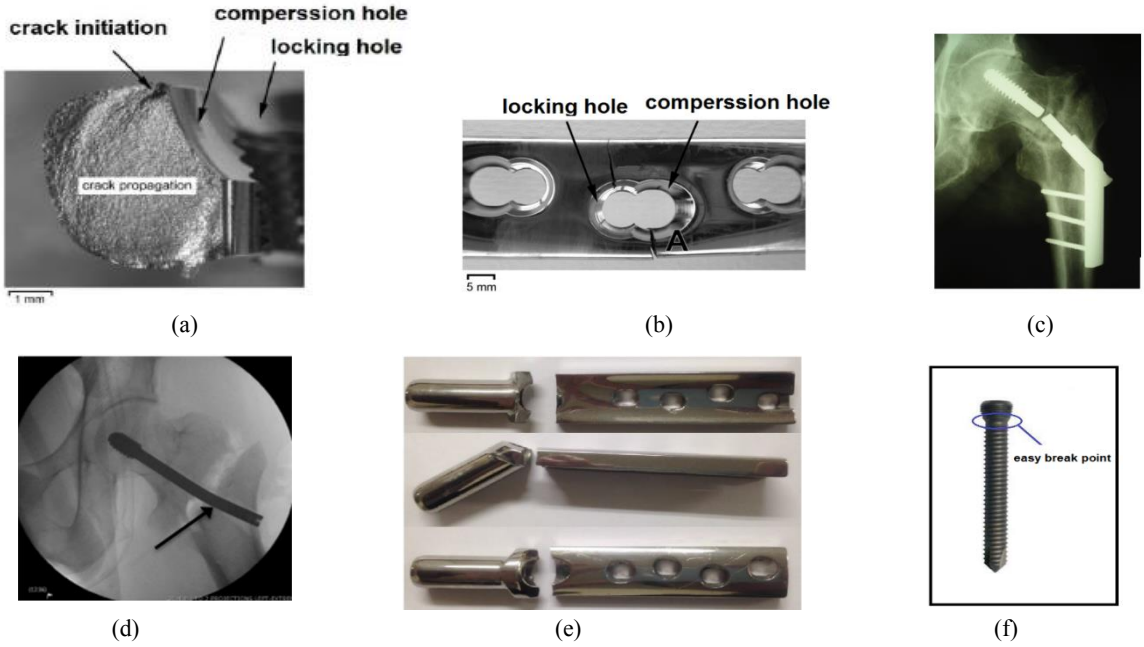

Fig.10
Some failure in DHS, (a) crack initiation in hole [10], (b) hole [10], (c) lag screw [17],(d) bending lag screw [18],(e) plate [32],(f) cortical screw[19].

In the present study, the trend of the amount of stress and strain in different parts of DHS is the same as the previous research [16, 28, 35, 36, 39]. According to Figs. 5, 6, 7, and Table 4, the maximum Von Mises stress (σ_{V-Max}) and ε_{V-Max} for DHS (both alloys) is happening in cortical screws, plate, compression screw, and lag screw, respectively. For both alloys, the range of σ_{V-Max} in cortical screws are between 134-196 *MPa*, in plate 138-175 *MPa*, in compression screw 124-155 *MPa*, and lag screw 121-150 *MPa* while the amount of σ_{V-Max} in the SS is between 25 to 32% more than Ti6. Comparing the results of the present study in case of static analysis by FEM with the research mentioned indicates large similarities in the trend of stress and strain changes, however, there are sometimes large differences in values. In [16], the amount of forces applied (large muscular forces), the mechanical properties of the alloy and bone differ from the present study, however, σ_{V-Max} in the lag screw, plate and cortical screws are 159, 91 and 321 *MPa*, respectively, while, in the present study, they are 155, 175 and 191 *MPa*, so cortical screws are critical points. Despite the difference in σ_{V-Max} due to different E, $\Delta\varepsilon_{V-Max}$ is very little (less

than 0.003%). In the [28], which examined two alloys similar to the present study, despite the difference in σ_{V-Max}, and ε_{V-Max}, the cortical screws (distal screws) were introduced as critical points, as in the present study. Also, the difference in σ_{V-Max} between the two alloys is about 20 to 23 %, which is very similar to the present study although like [16] there are differences in the assumptions. The stress and strain range is very low (concentration stress points are not seen in the contours) and the values are the same as the average stress in Table 5.

In [35], in addition to the differences mentioned in the assumptions of the present study and [16, 28], cortical screws are assumed threadless. For this reason, the most critical points are obtained on the lag screw and plate (zone 2 in Fig. 5(c)). According to the failure patterns reported in DHS [11, 17, 18, 33, 38], this zone has been mostly damaged, and the reason for the limited report of cortical screw failure in the real state can be explained by the corrosion, wear and adhesive of bone. Accordingly, the concentration stress points of the threads are adapted to the surrounding environment after a while and leave the stress concentration state [41, 42, 43]. In [36], although there are many differences in the subject assumptions by the present study, cortical screws are shown as a critical area and compression screw has lowest σ_{V-Max} like present study. Also in [39] $\sigma_{V-Max}=850MPa$ and $\varepsilon_{V-Max}=0.95\%$ in lag screw have a huge difference with the present study, which is due to the small size DHS, threadless screws and huge forces (200% higher than present study). All the mentioned assumptions play a decisive role in the amount and location of critical stress. In the present study, unlike other studies, bone is assumed to be an anisotropic material, and this issue makes its amount and strain obtained for bone different and reality from other studies. On the other hand, the amount of applied forces in the present study is the average value obtained from previous studies, which has made the amount of results different from other studies. The geometric characteristics of the bone and the implant are different in each study (case report), and therefore the results will certainly be different. The role of muscular forces is the determining factor in the amount of maximum stress and strain, and the choice of applied force model based on different research causes fundamental changes in the amount of critical stress. For example, in [39], one of the muscle forces was applied by three vectors (equivalent vectors), which caused a large change in the amount of stress. A small change in the mechanical properties of the alloys also has a significant effect on the critical stress value [28]. The placement of the implant in the femur and the right angle (135°) has a great effect on tension. For example, placing the implant in the right place on the neck of the femur (middle third) helps to reduce tension [33].

4.2 Analysis of fatigue results

Table 5 shows the life and σ_a of DHS components for triple activity (NW, DS, FA) in both alloys, in which the trend of life changes with the type of activity and alloy in different places of the DHS. According to the authors, no studies are simulating the determined life of components under different loading by FEA, and the present study is considered innovative in this respect. There are a few studies [10, 11, 12, 13, and 19] in terms of biomechanical analysis, which are very different in assumptions that govern the problem (like the static section). The life of the components when using the SS is about 30% less than Ti6, but this value is more or less in some locations. In the present analysis, due to the three activities in the way of applying force, the forces are assumed based on zero-based mode, because stepping is not like putting and removing force, and the tensile and compressive modes do not occur. If the reverse force method is used, the results of infinite lifespan are reduced to a finite life, which of course is not physically correct. Also, the frequency application for laboratory testing for titanium base alloys is usually from $5Hz$ to $20Hz$. In the present study, a frequency between 0.5 and 2 has been applied to the triple activity.

In study [10], the plate of DHS (lock plate) was subjected to a laboratory biomechanical test; although there are differences in the assumptions (alloy, force, left leg,...) with the present study, the location of the implant failure (Fig. 10(a)) is the same part that was obtained from the results of the present study (Fig. 6(d), Fig. 8(d)). These concentration stress points have been damaged by crack growth due to fatigue. The result of [11] which was performed biomechanically and clinically on three implant specimens, reports periods of 2 to 10 months for failure in zone 1 and 2 (Fig. 6(b), Fig. 10(b)). Two of the samples showed obvious signs of fatigue after metallography, which led to the initial local failure and loss of implant integrity; finally, the implant was removed from its proper place. In another case, improper implant design and inappropriate surgical technique have been reported to be the cause of failure. The commonalities of [11] with the present study are in terms of failure life in high cycles under low force (for two samples) and fatigue failure with low cycle (application of unforeseen large forces due to lack of proper surgery). In the study [12], a fatigue testing protocol was developed to evaluate the performance of constructs under cyclical loading by a newly designed locking plate which offers an alternative for treating challenging femoral neck fractures. There are differences in the type of implant (very small size three cancellous screws LCP), alloy and

loading conditions (2.47W) with the present study. However, the results of [12] are comparable to the present study because it indicates that the screws (207000 cycles) break faster than the plate (500000 cycles). In the present study, using the capabilities of Commercial finite element analysis software (nodal force calculation), it was found that the applied force on the femur (p_1) is about 45-55% of the applied force on the head of the lag screw. In [13], a laboratory test was performed to obtain the fatigue curve of the DHS in the lag screw. The main force applied to the head of the lag screw is 160 kg (equal to 349W %), which causes the lag screw to break in about 10^4-10^5 cycles. This test was without the presence of muscular and abductor forces, but the amount of the failure cycle is similar to the FA mode in the present study (Table 5). Research shows that for patients who have not yet recovered, the application of high forces causes the DHS to fail, and therefore, a rest period of at least two months is prescribed for patients. Obviously, postoperative life has special conditions for this group of patients, and performing operations such as jumping or falling causes irreparable injuries. The concentration points of the stress obtained FE in the present study are the same as the failure points (Fig. 10) in biomechanical, clinical, and laboratory research. Although cortical screws are assumed to be non-threaded in some studies, in the same studies, they have maximum high stress at the junction with the plate. The six critical zones in the static section, along with the holes of the plate, are common points of DHS failure. Fatigue cracks have been observed even in the lower cycles due to unforeseen forces (due to improper design) [10].

5 CONCLUSIONS

In the present study, a multi-part DHS (four holes) with two alloys (Ti6, SS) in static and fatigue modes was investigated. To select the forces on the femur, previous studies were investigated in some modes like walking slowly (such as standing), walking normally, down stairs, and falling. Because most research on DHS has been on specific and different patients with biomechanical, laboratory, and clinical methods, in addition, differences in the conditions of application of force, geometry, and alloy material have made the research results not comparable (in terms of quantity). By FEA, there is a lot of research in the static mode, but there is rare research on the fatigue mode. One of the highlights of the present study is the consideration of anisotropic bone while, in most studies, it is assumed to be isotropic. Also, the life and alternating stress on DHS components were obtained under the influence of different forces, and the authors believe that the present study could be a basis for future research from this point of view. The achievements of the present study, as follows, can determine the dimensions of this article:

- In static mode, σ_{V-Max} and ε_{V-Max} occurs in the DHS components, respectively in the cortical screws, plate, compression screw, and lag screw.
- In static mode, $\sigma_{V-Max}=145MPa$ in Ti6 is about 30% lower than the SS ($\sigma_{V-Max}=196MPa$), also $\varepsilon_{V-Max}=0.191$ in Ti6 is higher than the SS ($\varepsilon_{V-Max}=0.121$).
- In static mode, the femur (intertrochanteric region) with $\varepsilon_{V-Max}=0.277$ has maximum strain.
- Obtaining critical points in static analysis that shows a similar trend in stress and strain to previous research.
- Critical points in static and fatigue analysis are the same.
- In fatigue analysis, DHS components with Ti6 alloy have infinite life in NW, DS activity, and only in FA activity has a finite life (10^7-10^8 cycle) with $\sigma_{amax}=425MPa$ in cortical screw.
- In fatigue analysis, DHS components with SS alloy have a finite life in all activity, which $NW\sim10^7 cycle, DS\sim10^6 cycle$ and even in cortical screw, the life of failure reaches 98 cycles with $\sigma_{amax}=486MPa$ in FA activity.
- The proportion of σ_{amax} changes in NW is 18-23% lower than in DS and for DS is 48-53% lower than FA activity.
- The critical regions that are obtained by FEA are the same as the failure regions common in previous biomechanics and clinical studies. These regions are mainly concentration stress points that lead to DHS failure as the crack grows.
- In the present study, unlike other studies, bone is assumed to be an anisotropic material.

REFERENCES

[1] Teoh S.H., 2000, Fatigue of biomaterials: a review, *International Journal of Fatigue* **22**: 825-837.

[2] Niinomi M., Nakai M., 2011, Titanium-based biomaterials for preventing stress shielding between implant devices and bone, *International Journal of Biomaterials* **2011**: 836587.

[3] Tokaji K., 2006, High cycle fatigue behavior of Ti–6Al–4V alloy at elevated temperatures, *Scripta Materialia* **54**: 2143-2148.

[4] Janecek M., Novy F., Harcuba P., Strasky J., Trkoc L., Mhaeded M., Wagnerd L., 2015, The very high cycle fatigue behavior of Ti_6Al_4V alloy, *Acta Physica Polonica A* **128**: 497-502.

[5] Agius D., Kourousis K.I., Wallbrink C., 2018, A review of the As-Built SLM Ti-6Al-4V mechanical properties towards achieving fatigue resistant designs, *Metals* **8**(1): 75.

[6] Berrios J.A., Teer D.G., Puchi-Cabrera E.S., 2001, Fatigue properties of a 316L stainless steel coated with different TiN*xn* deposits, *Surface and Coatings Technology* **148**: 179-190.

[7] Huang J.Y., Yeh J.J., Jeng S.L., Chen C.Y., Kuo R.C., 2006, High-cycle fatigue behavior of type 316L stainless steel, *Materials Transactions* **47**(2): 409-417.

[8] Berrios-Ortiz J.A., La Barbera-Sosa J.G., Teer D.G., Puchi-Cabrera E.S., 2004, Fatigue properties of a 316L stainless steel coated with different ZrN Deposits, *Surface and Coatings Technology* **179**: 145-157.

[9] Lei Y.B., Wang Z.B., J.L. Xu J.L., Lu K., 2019, Simultaneous enhancement of stress- and strain-controlled fatigue properties in 316L stainless steel with gradient nanostructure, *Acta Materialia* **168**:133-142.

[10] Kanchanomai C., Phiphobmongkol V., Muanjan P., 2008, Fatigue failure of an orthopedic implant – a locking compression plate, *Engineering Failure Analysis* **15**: 521-530.

[11] Spivak J.F., Zuckerman J.D., Kummer F.J., Frankel V.H., 1991, Fatigue failure of the sliding screw in hip fracture fixation: a report of three cases, *Journal of Orthopaedic Trauma* **5**(3): 325-331.

[12] Hunt S., Martin R., Woolridge B., 2011, Fatigue testing of a new locking plate for hip fractures, *Journal of Medical and Biological Engineering* **32**(2): 117-122.

[13] Regazzoni P., Rüedi Th., Winquist R., Allgöwer M., 1985, *The Dynamic Hip Screw Implant System*, Springer-Verlag Berlin Heidelberg.

[14] Wierszycki M., Kąkol W., Lodygowski T., 2006, Fatigue algorithm for dental implant, *Foundations of Civil and Environmental Engineering* **7**: 363-380.

[15] Kouvidis G.K., Sommers M.B., Giannoudis P.V., Katonis P.G., Bottlang M., 2009, Comparison of migration behavior between single and dual lag Screw implants for intertrochanteric fracture fixation, *Journal of Orthopaedic Surgery and Research* **4**: 16.

[16] Siamnuai K., Rooppakhun S., 2012, Influence of plate length on the Mechanical performance of dynamic hip screw, *International Association of Computer Science and Information Technology Singapore* **23**: 48-52.

[17] Necas L., Hrubina M., Cibula Z., Behounek J., Krivanek S., Horak Z., 2017, Fatigue failure of the sliding hip screw – clinical and biomechanical analysis, *Computer Methods in Biomechanics and Biomedical Engineering* **20**: 1364-1372.

[18] Arastu M.H., Phillips L., Duffy P., 2013, An unusual failure of a sliding hip screw in the immediate post-operative period, *Injury Extra* **44**: 23-27.

[19] Tian X., Yabo L., 2016, Screw layout optimization to solve fatigue fracture of femoral Ti alloy metal plate, *International Symposium on Materials Application and Engineering* **67**: 03019.

[20] Sheikh M.S.A., Ganorkar A.P., 2015, Optimization of femoral intramedullary nailing using finite element analysis , *International Journal for Innovative Research in Science & Technology* **2**(4): 123-125.

[21] Bergmann G., Deuretzbacher G., Heller M., Graichen F., Rohlmann A., Strauss J., Duda G.N., 2001, Hip contact forces and gait patterns from routine activities, *Journal of Biomechanics* **34** : 859-871.

[22] Schwachmeyer V., Damm P., Bender A., Dymke J., Graichen F., 2013, In vivo hip joint loading during post-operative physiotherapeutic exercises, *PLoS ONE* **8**(10): e77807.

[23] Farhoudi H., Oskouei R.H., Zanoosi A.A.P., Jones C.F., Taylor M., 2016, An analytical calculation of frictional and bending moments at the head-neck interface of hip joint implants during different physiological activities, *Materials* **9**(12): 982.

[24] Simoes J.A., Vaz M.A., Blatcher S., Taylor M., 2000, Influence of head constraint and muscle forces on the strain distribution within the intact femur, *Medical Engineering and Physics* **22**: 453-459.

[25] Modenese L., Montefiori E., Wesarg S., Viceconti M., 2018, Investigation of the dependence of joint contact forces on musculotendon parameters using a codified workflow for image-based modelling, *Journal of Biomechanics* **73**: 108-118.

[26] Chalernpon K., Aroonjarattham P., Aroonjarattham K., 2015, Static and dynamic load on hip contact of hip prosthesis and thai femoral bones, *International Journal of Mechanical and Mechatronics Engineering* **9**: 251-255.

[27] Eschweiler J., Fieten L., Anna J.D., Kabir K., Gravius S., Tingart M., Radermacher K., 2012, Application and evaluation of biomechanical models and scores for the planning of total hip arthroplasty, *Journal of Engineering in Medicine* **226**(12): 955-967.

[28] Taheri N.S., Blicblau A.S., Singh M., 2011, Comparative study of two materials for dynamic hip screw during fall and gait loading: titanium alloy and stainless steel, *Journal of Orthopaedic Science* **16**: 805-813.

[29] Orías A.A.E., Deuerling J.M., Landrigan M.D., Renaud J.E., Roeder R.K., 2009, Anatomic variation in the elastic anisotropy of cortical bone tissue in the human femur, *Journal of* the *Mechanical Behavior* of *Biomedical Materials* **2**(3): 255-263.

[30] Vignoli L., Kenedi P.P., 2016, Bone anisotropy – analytical and finite element analysis, *Latin American Journal of Solids and Structures* **13**(1): 51-72.

[31] Korsa R., Mares T., 2012, Numerical identification of orthotropic coefficients of the lamella of a bone's osteon, *Bulletin of Applied Mechanics* **8**(31): 45-53.

[32] Chang C.W., Chen Y.N., Li C.T., Peng Y.T., Chang C.H., 2015, Role of the compression screw in the dynamic hip–screw system :A finite-element study, *Medical Engineering and Physics* **37**: 1174-1179.

[33] Hrubina M., Horák Z., Bartoška R., Navrátil L., Rosina J., 2013, Computational modeling in the prediction of dynamic hip screw failure in proximal femoral fractures, *Journal of Applied Biomedicine* **11**: 143-151.

[34] Cun Y., Dou C.H., Tian S., Li M., Zhu Y., Cheng X., Chen W., 2020, Traditional and bionic dynamic hip screw fixation for the treatment of intertrochanteric fracture: a finite element analysis, *International Orthopaedics* **44**: 551-559.

[35] Çelik T., Mutlu I., Ozkan A., Kisioglu Y., 2019, The evaluation of the relation between dynamic hip screw positions and its failure in unstable femur fractures, *Australian Journal of Mechanical Engineering* **19**: 261-267.

[36] Kajzer W., Prajsnar G., Kajzer A., Rodak L., Marciniak J., Mielnik M., Semenowicz J., Hermanson J., Koczy B., 2017, *Application of Dynamic Hip Screw System in Treatment of Intertrochanteric Fracture*, Innovations in Biomedical Engineering.

[37] Viceconti M., Casali M., Massari B., Cristofolini L., Bassinit S., Tonis A., 1996, The 'standardized femur program' proposal for a reference geometry to be used for the creation of finite element models of the femur, *Journal of Biomechanics* **29**(9):1241.

[38] Nica M., Cretu B., Ene D., Iulian Antoniac I., Gheorghita D., Ene R., 2020, Failure analysis of retrieved osteosynthesis implants, *Materials* **13**(5): 1201.

[39] Zeng W., Liu Y., Hou X., 2020, Biomechanical evaluation of internal fixation implants for femoral neck fractures: A comparative finite element analysis, *Computer Methods and Programs in Biomedicine* **196**: 105714.

[40] Heller M.O., Bergmann G., Kassi J.-P., Claes L., Haas N.P., Duda G.N., 2005, Determination of muscle loading at the hip joint for use in pre-clinical testing, *Journal of Biomechanics* **38**: 1155-1163.

[41] Santos C.T.D., Barbosa C., Monteiro M.D.J., Abud I.D.C., Caminha I.M.V., Roesler C.R.D.M., 2015, Fretting corrosion tests on orthopedic plates and screws made of ASTM F138 stainless steel, *Research on Biomechanical Engineering* **31**(2): 169-175.

[42] Lee C.C., Lin S.C., Kang M.J., Wu S.W., Fu P.Y., 2010, Effects of implant threads on the contact area and stress distribution of marginal bone, *Journal of Dental Sciences* **5**(3): 156-165.

[43] Kuroda S., Tanaka E., 2014, Risks and complications of mini screw anchorage in clinical orthodontics, *Japanese Dental Science Review* **50**: 79-85.